Chapter 12

# Adaptive Robust Control of Biomass Fuel Co-Combustion Process

Konrad Gromaszek and Andrzej Kotyra

Additional information is available at the end of the chapter

http://dx.doi.org/10.5772/intechopen.71576

**Abstract**

The share of biomass in energy production is constantly growing. This is caused by environmental and industry standards and EU guidelines. Biomass is used in the process of co-firing in large power plants and industrial installations. In the existing power stations, biomass is milled and burned simultaneously with coal. However, low-emission combustion techniques, including biomass co-combustion, have some negative side effects that can be split into two categories. The direct effects influence the process control stability, whereas the indirect ones on combustion installations via increased corrosion or boiler slagging. The effects can be minimised using additional information about the process. The proper combustion diagnosis as well as an appropriate, robust control system ought to be applied. The chapter is devoted to the analysis of modern, robust control techniques for complex power engineering applications.

**Keywords:** adaptive control, model predictive control, complex system, co-combustion, energy, controllability, robust

## 1. Introduction

Regarding the fact that coal is still themain fuel used in electricity generation around the world and it contains impurities that significantly increase pollutant emissions, new combustion techniques are developed, e.g. air staging, reburning and flue gas circulation [1]. Fossil fuel depletion forces the use of renewable fuels such as biomass; in existing power stations, biomass is milled and burned simultaneously with coal. However, low-emission combustion techniques, including biomass co-combustion, have negative effects: directly influence on process control stability/efficiency and indirectly on combustion installations via increased corrosion or boiler slagging [2]. These effects can be minimised using additional information about the process that makes combustion monitoring (diagnosis) system necessary to apply [3].

The combustion efficiency of pulverised fuel depends on several parameters. The commonly applied, low-emission techniques use recirculation vortexes that lengthen the paths of the coal grains passing through the flame to minimise generation of thermal oxides of nitrogen ($NO_x$). To make co-combustion of pulverised coal more efficient and environment-friendly, it is necessary to measure its key parameters.

The information taken at the output is delayed and averaged. Although there are several combustion diagnostic direct techniques, the most of them are expensive or impossible to utilise under industrial conditions. The radiation emitted by the flame reflects the combustion process occurring in chemical reactions and physical processes. The fast and minimally invasive optical methods allow to use image processing-based information in process control system. Such approach gives non-delayed and spatially selective additional information about the ongoing combustion process. The still and apparent position of flame is the result of dynamic equilibrium between the local flame propagation speed and the speed of the incoming fuel mixture. It allows assuming that the shape of a flame can be an indicator of the combustion process, occurring under certain conditions.

As a result, the relationship between the parameters describes the variation of the flame and the temperature of the exhaust gas in the chamber or the amount of air flow in the secondary factor. Thus, if the temperature is slowly varying value, having an inert nature, the reasonable approach is including a single or a set of the image parameters that would provide fast information to the synthesis of the controller. Due to the incomplete knowledge about the control plant or various changes in its performance, the control system with fixed parameters is insufficient. Then, it is recommended to use the adaptive control approach. The required knowledge of the complex nonlinear object may be achieved using different methods but due to the process, they ought to be robust and secure. It seems to be a very interesting application for robust adaptive control algorithms.

## 2. Process models and uncertainties

Every detailed aspect of the real process cannot be adequately contemplated by mathematical models. Simplifying assumptions have to be made, especially due to the control purposes, where models with simple structures and sufficiently small size have to be used regarding to the available control techniques and real-time considerations. Therefore, mathematical control models can only describe the dynamics of the process in an approximate way.

Majority of modern control techniques need a control model of the plant with fixed structure and parameters, which is used throughout the design stage. For an exact description of the plant (neglecting external disturbances), processes could be controlled by an open-loop controller. However, feedback is necessary for process control because of the external perturbations and model inaccuracies in all real processes.

The objective of robust control is to design controllers which preserve stability and performance in spite of the modelling inaccuracies or uncertainties. Although the use of feedback contemplates the

inaccuracies of the model simplicity, the term of robust control is used in [4, 5] to describe control systems that explicitly consider the discrepancies between the model and the real processes.

Depending on the technique used to design the controllers, there are different approaches in modelling uncertainties. The most extended techniques are frequency response uncertainties and transfer function parametric uncertainties. Most of the cases assume that the plant can be exactly described by one of the models belonging to a family. That is, if the family of models is composed of linear models, the plant is also linear. In case of model predictive control (MPC) approach, the uncertainties can be defined about the prediction capability of the model.

Frequency uncertainties are usually described by a band around nominal frequency response. The plant frequency response is presumed to be included in the band. In case of parametric uncertainties, each coefficient of the transfer function is presumed to be bounded by uncertainties limit. The plant is then presumed to have a transfer function with parameters within the uncertainty set. There is an assumption that the plant is linear with a frequency response within the uncertainty band for the first case and the plant is linear and of the same order as that of the family of models for the case of parametric uncertainties.

The control models in MPC are used to predict what is going to happen: future trajectories. The appropriate way to describe uncertainties in this context seems to be the model (or a set of models) that instead of generating a future trajectory may also generate the band of trajectories in which the process of trajectory will be included when the same input is applied, in spite of uncertainties. In case of availability of good process model, this band is narrow, and the uncertainty level is low.

The most general way of posing problem in MPC considers a process whose behaviour is dictated by the equation:

$$y(t+1) = f\big(y(t), \ldots, y\big(t-n_y\big),\ \ u(t), \ldots, u(t-n_u),\ \ z(t), \ldots, z(t-n_z), \psi\big) \tag{1}$$

where $y(t) \in \mathbf{Y}$ and $u(t) \in \mathbf{U}$ are $n$ and m vectors of outputs and inputs, $\psi \in \boldsymbol{\Psi}$ is a vector of parameters, possibly unknown, and $z(t) \in \mathbf{Z}$ is a vector of possibly random variables.

Consider the model or family of models, for the process described by:

$$\widehat{y}(t+1) = \widehat{f}\,(y(t), \ldots, y(t-n_{na}),\ \ u(t), \ldots, u(t-n_{nb}),\ \ \theta) \tag{2}$$

where $\widehat{y}(t+1)$ is the prediction of output vector for instant $t+1$ generated by the model $\widehat{f}$ is a vector function, usually simplification of $f$, $n_{na}$ and $n_{nb}$ are the number of past outputs and inputs considered by the model and $\theta \in \boldsymbol{\Theta}$ is a vector of uncertainties about the plant. Variables that are although influencing the plant dynamics are not considered in the model due to the necessary simplifications or for the other reasons are represented by the $z(t)$.

The dynamics of the plant in (1) are completely described by the family of models (2) if for any $y(t), \cdots, y(t-n_y) \in \boldsymbol{Y}$, $u(t), \cdots, u(t-n_u) \in \boldsymbol{U}$, $z(t), \cdots, z(t-n_z) \in \boldsymbol{Z}$ and $\psi \in \boldsymbol{\Psi}$, there is a vector of parameters $\theta_i \in \boldsymbol{\Theta}$ such that:

$$f\left(y(t),\ldots,y\left(t-n_y\right),\ \ u(t),\ldots,u(t-n_u),\ \ z(t),\ldots,z(t-n_z),\psi\right) = \widehat{f}\left(y(t),\ldots,y(t-n_{na}),\ \ u(t),\ldots,u(t-n_{nb}),\ \ \theta\right) \tag{3}$$

The way in which uncertainties parameter $\theta$ and its domain $\boldsymbol{\Theta}$ are defined mainly depends on the structures of $f$ and $\widehat{f}$ and on the degree of certainty about the model. The following are the most popular structures in MPC approaches [5]:

- Truncated impulse response uncertainties—Suitable when the plant model is nonlinear and linear (obtained at different operating regimes), so the plant is described by a linear combination q known stable linear time-invariant plants with unknown weighting $\theta_j$.
- Matrix fraction description uncertainties—Frequently, the state space description is used and each of the entries of the transfer matrix is characterised by its static gain, time constant and dead time. Bounds on the coefficients of matrices $\boldsymbol{A}(z^{-1})$ and $\boldsymbol{B}(z^{-1})$ can be obtained on the gain and time constants. However, uncertainties about the dead time are difficult to handle. If the uncertainty band about the dead time is smaller, the pure delay of the discrete-time model does not have to be changed. The fractional delay time can be modelled by the Pade expansion and the uncertainty bound of these coefficients can be calculated from the uncertainties of the dead time. It is imperfect for real-time applications due to min-max problem solving. If the uncertainties only affect polynomial matrix B, the prediction equation is an affine function of the uncertainty parameter and the resulting min-max problem is less computationally expensive.
- Global uncertainties—Based on assumption that all modelling errors are globalised in a vector of parameters, the process can be approximated by a linear model in the sense that all trajectories will be included in bands that depend on $\theta(t)$. If the process variables are bounded, the global uncertainties are also be bounded.

The objective of prediction control is to compute the future control sequence $u(\mathrm{t}), u(\mathrm{t}+1), \cdots, u(\mathrm{t}+N_u)$ in such way that the optimal j step ahead predictions $\mathrm{y}(\mathrm{t}+\mathrm{j}|\ \mathrm{t})$ are driven close to $\mathrm{w}(\mathrm{t}+\mathrm{j})$ for the prediction horizon. The way in which system approach the desired trajectories is indicated by the function $J$ which depends on the present and future control signals and uncertainties. Usually, for the stochastic type of the uncertainty, the function J minimization for the most expected situation, supposing that the future trajectories are going to be the future expected trajectories. In case bounded uncertainties are considered explicitly, bounds on the predictive trajectories can be calculated and more robust control would be obtained when controller tried to minimise the objective function for the worst situation, by solving:

$$\min_{u\in U}\ \max_{\theta\in\Theta} J(u,\theta) \tag{4}$$

The function to be minimised is the maximum of the norm that measures how well the process output follows the reference trajectories.

Different types of norms can be used for this purpose, e.g. quadratic cost function [6], ∞-∞ norm [7] or 1-norm [8].

In case quadratic cost function of $\theta$ for each value of $\boldsymbol{u}$, used Hessian matrix (see [6]) can be assured to be positive definite. This implies that the function is convex and there are no local optimal solutions different from the global optimal solution. One of the main problems of nonlinear programming algorithms, the presence of local minima, is avoided. Such an approach can be prohibitive for real-time applications with long costing and control horizons. Of course, the problem gets more complex when the uncertainties on the input and output parameters are considered.

Campo and Morari have proved that the ∞-∞ norm reduces min-max problem; therefore, it requires fewer computation and can be solved using standard algorithms. Although ∞-∞ norm seems to be appropriate in terms of robustness, it is only concerned with maximum deviation and the rest of the behaviour is not taken explicitly into account. Other types of norms are more adequate for measuring the performance. Alwright [8] has shown that this method can be extended to the 1-norm.

### 2.1. Robustness by imposing constraints

To guarantee robustness in MPC is imposing the stability conditions for all possible realisations of uncertainties [9]. The key ingredients of the stabilising MPC are a terminal set and a terminal cost. The terminal state (i.e. the state at the end of the prediction horizon) is forced to reach a terminal set that contains the steady state. An associated terminal cost is added to the cost function.

The robust MPC consists of finding a vector of future control moves such that it minimises an objective function (including a terminal cost satisfying the stability conditions [9]) and forces the final state to reach the terminal region for all possible values of uncertainties, that is:

$$\min_{u \in U} J(x(t), u) \text{ subject to} \forall \theta \in \Theta \begin{cases} \mathbf{Ru} \leq \boldsymbol{r} + \boldsymbol{V}x(t) \\ x(t+N) \in \Omega_{\mathrm{T}} \end{cases} \tag{5}$$

where the terminal set $\boldsymbol{\Omega}_T$ is usually defined by a polytope $\boldsymbol{\Omega}_T \triangleq \{x : \mathbf{R}_{T^x} \leq \mathbf{r}_T\}$. The inequality $\mathbf{Ru} \leq \boldsymbol{r} + \mathbf{V}x(t)$ contains the operating constraints. If there are operating constraints on the process output and/or state, vector $\mathbf{r}$ is an affine function of the uncertainties $\theta$.

In general, industrial processes are nonlinear, but most of MPC applications are based on the use of linear models. There are two reasons for this:

- The identification of a linear model based on process data is relatively easy.
- Linear models provide good results when the plant is operating in the neighbourhood of the operating point. In the MPC appliances, the objective is to keep the process around the stationary state rather than perform frequent changes from one operating point to another, and therefore, a precise linear model is enough. The use of linear model together with a quadratic objective function gives rise to a convex problem whose solution is well studied and implemented in many commercial products. The existence of algorithms that can guarantee a convergent solution in a time shorter than sampling time is crucial in processes with the great number of variables.

However, the dynamic response of the resulting linear controllers is unacceptable when applied to processes that are nonlinear to varying degrees of severity. Despite the fact that in many situations the process will be operating in the neighbourhood of a steady state, and therefore a linear representation will be adequate, there are some very important situations where it does not occur. There are processes for which the nonlinearities are so severe and so crucial to the closed loop stability that a linear model is not sufficient.

## 3. Robust control of biomass fuel co-combustion

The design of stabilising controllers for nonlinear controllers with known and unknown constant parameters has significant improvement within the last decades. It involves design techniques such as adaptive feedback linearization [10–12], adaptive backstepping [13–15], robust Lyapunov functions (CLFs and RCLFs) [16–19], nonlinear damping and swapping [14, 20] as well as switching adaptive control [21, 22]. They are applicable for globally stabilising controllers for single input feedback linearizable systems [10, 11, 22] and parametric-strict-feedback systems [13–15]. Despite this, the problem of adaptive control of a big class of nonlinear systems still remains unexplored.

The procedure presented in Ref. [23] for designing robust adaptive controllers for a large class of multi-input nonlinear systems with exogenous bounded input disturbances results in approach that combines the theory of control Lyapunov functions and the switching adaptive controller to overcome the problem of computing the control law in the case where estimation model becomes uncontrollable.

It is important that the control law depends on estimates of the Lie derivative $L_gV$, which depends both on the system vector-fields and robust control Lyapunov function (RCLF) $V$. The class of systems for which the proposed approach is applicable can be characterised by the following assumption: $L_gV$ depends linearly on unknown constant parameters, where $g$ denotes the input vector field and $V$ is CLF (RCLF) for the system.

Contrary to the classical adaptive approach where the control law depends on estimates of the system vector-fields, in the presented case, it depends on estimates of the RCLF term [23]. $L_gV$ depends on both system vector-fields and RCLF function $V$.

On the one hand, the main advantage of such approach is that Lyapunov inequalities relating to the parameter estimation errors and the time derivative of the RCLF are easy to handle. But on the other hand, the designed controllers depend critically on the knowledge of $L_gV$. In case of adaptive versions of such controllers, there is the risk of failure regarding to the fact that the estimate of $L_gV$ may have a different sign at certain times than the actual $L_gV$. Similarly, when the estimate of $L_gV$ is close to zero, the actual $L_gV$ is not. Such divergences imply uncontrollability of the estimation model, even if the actual model is not.

To overcome these problems, the switching control law is used, which is modified version of control law presented in Ref. [22]. Such control law approximately switches between two adaptive controllers, which have the following properties: (1) both controllers behave approximately

the same in the nonadaptive case and (2) when one of these controllers becomes nonimplementable, the other one is implementable.

The proposed approach is significant because it constructs globally stabilising controllers for a wider class of plants than *multi-input feedback linearizable systems* and *parametric-pure-feedback systems* and can be expressed as:

$$\dot{x} = Fx + G\left[\vartheta_1^{\tau} l_0(x) + \vartheta_2^{\tau} l_1(x)\right]u, \tag{6}$$

where $x \in \Re^n$ and $u \in \Re^m$ denote the state and the control input vectors, $F$, $G$, $\vartheta_i$, $i = 1, 2$ are constant unknown matrices and $l_0$, $l_1$ are continuous matrix functions, non-singular for all $x$.

The existing adaptive designs guarantee [10–12] closed-loop stability only if the constant matrices $G$, $\vartheta_2$ are known.

In case of the parametric-pure-feedback system, denoted by:

$$\begin{aligned} \dot{x}_1 &= x_{i+1} + \theta^T f_i(x_i, \ldots, x_{i+1}) \quad 1 \le i \le n-1 \\ \dot{x}_n &= \theta^T f_n(x) + \left[\theta^T g_{n2}(x) + g_{n1}(x)\right]u' \end{aligned} \tag{7}$$

where $\theta$ is a vector of unknown constant parameters, $x$ denotes the state vector of the system and $f_i$, $g_{ni}$ are continuous functions. The global stability procedures, presented in [13, 15, 20], guarantee the global stability only if the input vector field $\theta^T g_{n2}(x) + g_{n1}(x)$ is independent $\theta$ and the functions $f_i$ are independent of $x_{i+1}$.

For the problem formulation, the nonlinear system of the following form is considered:

$$\dot{x} = f(x) + g(x)u + g_w(x)w, \tag{8}$$

where $x \in R^n$, $u \in R^m$ and $w \in R^k$ denote vectors of system states, control inputs and disturbances and f, g, $g_w$ are $C^1$ vector-fields of appropriate dimensions. We assume that the disturbance vector w is bounded. The control objective is to find the control input u as a function of x such that all closed-loop signals are bounded and $x \to 0$ as $t \to \infty$. Since $w(t) \neq 0$, $t \ge 0$ and is assumed to be any general unknown bounded continuous time function.

The system (8) is robustly asymptotically stabilizable (RAS) when there exists a control law $u = k(x)$, where $k$ is appropriate feedback, such that the closed-loop solutions are robustly globally uniformly asymptotically stabilizable (RGUAS), according to definitions given in [16, 24].

Other approaches involve artificial intelligence methods to guarantee robust adaptive control for MIMO nonlinear systems. Fuzzy logic controllers have proven to have great potential in applications to complex or poorly modelled systems. Wang and Mendel in [25, 26] have started studies regarding fuzzy control of uncertain nonlinear systems. According to Wang [26], it is possible to find control law to achieve a stable control loop system. Chiu [27] proposed a universal fuzzy approximator for feedback cancellation, and the stability is guaranteed by Lyapunov's method. While the system is composed of tunable fuzzy sets, the approach is called Mamdani fuzzy approximation (MFA) control. Such a MFA controller is often extended

to robust adaptive controllers due to [28, 29], but this requires a large number of fuzzy rules to achieve satisfactory approximator. To cope this problem, in [30–33], Takagi-Sugeno fuzzy approximator (TSFA) is involved. The invertible fuzzy approximated input matrix needs to be imposed in case of MIMO systems [34–36]. Furthermore, some examples of combining fizzy adaptive and sliding mode control can be found in [37, 38]. The examples of robust fuzzy adaptive control schemes with guaranteed H∞ control performance for a specific class of MIMO nonlinear systems can be found in [39–41].

## 4. Flame images-based biomass-coal combustion characterisation

The efficiency of pulverised fuel depends on several parameters. The commonly applied, low-emission techniques of pulverised coal combustion use recirculation vortexes that lengthen the paths of the coal grains passing through the flame to minimise generation of thermal oxides of nitrogen ($NO_x$). To make pulverised coal combustion more efficient and environment friendly, it is necessary to measure its key parameters. The information taken from the output (exhaust gas collector) is delayed and averaged. In Ref. [42], several combustion diagnostic direct techniques are presented; the most of them are impossible to utilise under industrial conditions or are expensive. Fast and minimally invasive optical methods allow using image processing-based information in process control system [43].

Combustion tests were done in a 0.5 MWth (megawatt of thermal) research facility, enabling scaled down (10:1) combustion conditions with a swirl burner. The cylindrical shape combustion chamber has the following dimensions: 2.5 m long and 0.7 m in diameter. There is a low-$NO_x$ burner mounted horizontally at the front wall with 0.1 m in diameter. The stand has the necessary fuel supply systems: primary and secondary air, coal and oil. Previously prepared pulverised coal is dumped into the coal feeder bunker. Additionally, after passing through the feeder, straw is mixed with coal.

Two lateral inspection openings on both sides of the combustion chamber provide image acquisition. The CMOS sensor-based high-speed camera was placed near burner's nozzle (see **Figure 1**), because this area was considered as the crucial one. The 0.7 m length borescope was engaged in the transfer of the flame images from the inside of the combustion chamber. The camera acquired up to 500 frames per second at its maximal resolution (1280 × 1024 pixels). The optical system was cooled with water jacket. Additionally, purging air was used to avoid dustiness of optical elements of the probe.

To comply with standards, the combustion test included the following steps. First, the combustion chamber was warmed up by burning oil. After reaching the proper temperature level, the oil supply was switched off [44], and coal and biomass mixture supplied by the primary air was delivered to the burner. While the primary air was used for fuel feeding, the excess air coefficient was determined through the secondary air flow.

Several variants were taken into consideration, where thermal power ($P_{th}$) and excess air coefficient ($\lambda$) were set independently for known biomass content. It is notable that the $\lambda$ was defined as quotient the mass of air to combust 1 kg of fuel to the mass of stoichiometric air.

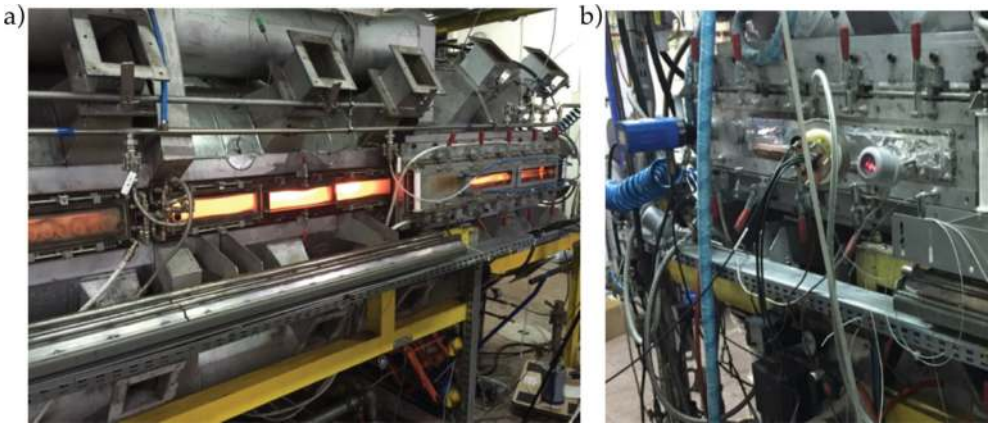


**Figure 1.** View of combustion facility: (a) left side, (b) right side with the installed camera.

The study was conducted for three exact thermal power values (250, 300 and 400 kW) at the object's output and certain excess air coefficient (0.65, 0.75, and 0.85).

The tests covered two fuel mixtures containing 10% and 20% of biomass (straw), respectively. The research assumed that biomass physical properties (like particle size, inherent moisture, etc.) as well as all the image acquisition parameters (such as frame rate, camera gain and exposure time) remained unchanged. Flame images acquisition covered different fuels mixtures in every variant of the combustion facility. In order to guarantee online algorithm controllability, the images pixel amplitude was limited to 0–255 range due to 8-bit grayscale conversion. The flame area within each frame of the acquired image sequence was determined on the basis of pixel amplitude to distinguish the flame as far brighter than any other registered objects within the field of view of the borescope. Thus, a sum of all the pixels contained within the bright region defined the flame area. Coordinates of flame area centre (x, y) are calculated as the mean value of the line or column coordinates, respectively, of all flame area pixels. Flame contour length was defined as a sum of all boundary pixels, assuming that the distance between two neighbouring contour points parallel to the coordinate axes is rated 1.

Changes of flame area that were obtained for fuel mixtures with 10% and 20% content of biomass obtained for different values of thermal power and excess air coefficient are presented in **Figures 2** and **3**, respectively. Every combustion state defined by set of constant values of $P_{th}$, $\lambda$, and biomass content was represented by 2000 images.

Raise of thermal power of combustion facility causes increasing of flame area, as shown in **Figures 2a** and **3a**.

Rise of thermal load also affects coordinates of the flame area centre, especially the x-coordinate for coal with 10% of biomass only indicating that the distance between flame front and burner nozzle increases (**Figure 2c**). For the other fuel mixture tested, the flame position was more stable (**Figure 3c** and **d**).

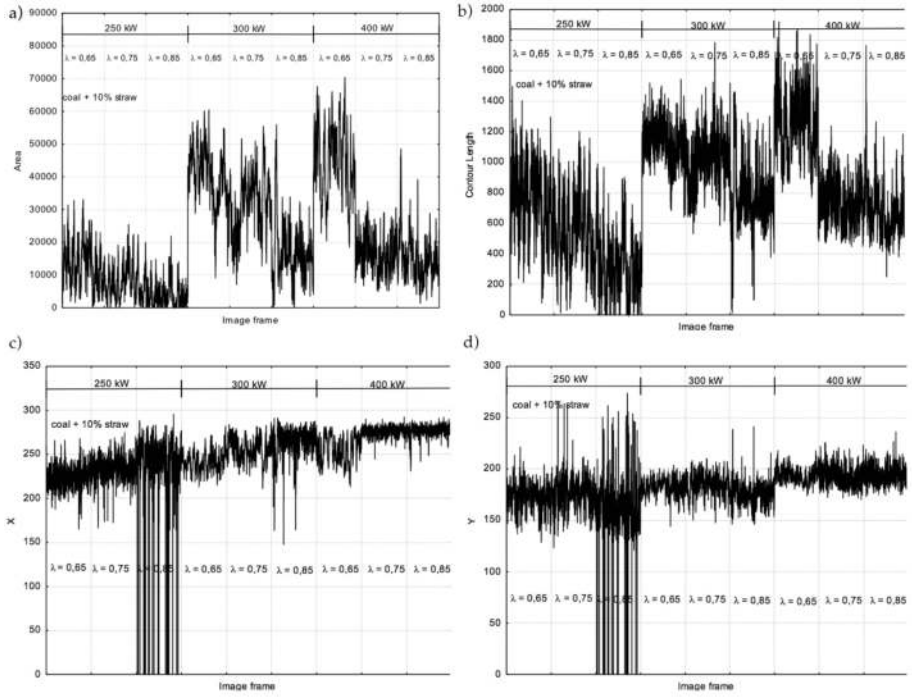


**Figure 2.** Flame area (a), contour length (b) and coordinates of flame area centre (c and d) obtained for different states of combustion process—coal with 10% content of biomass.

Low values of the flame area and contour length as well as sudden drops of coordinates of flame centre area observed for $P_{th}$ = 250 kW and $\lambda$ = 0.85 point to stability problems, which occurred during combustion tests.

Another important factor is variability of the flame parameters discussed, that were calculated for each combustion state.

Amount of excess air coefficient significantly affects combustion process. However, the mean value of flame area has different dependencies on $\lambda$ for the different values of thermal power. For $P_{th}$ = 400 kW, the flame area decreases when excess air coefficient increases for fuel mixtures with 10% and 20% of biomass.

Variability of flame contour length is almost the same as it does in the case of flame area.

Changes of the flame centre position are different for the examined variants. For biomass content of 20%, the standard deviation of the discussed parameter is greater, especially for greater $\lambda$ and thermal power value.

Comparing the mean values of flame area for the same excess air coefficient, it could be observed that flame area is larger for fuel mixtures with higher biomass content. This is because biomass contains more volatile contents comparing to coal.

http://dx.doi.org/10.5772/intechopen.71576

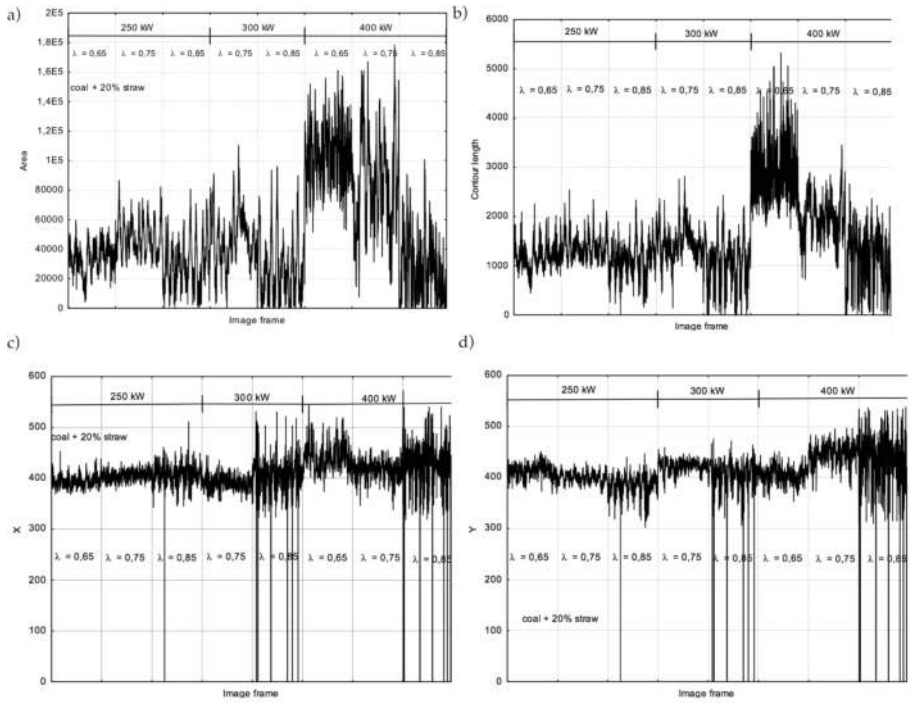


**Figure 3.** Flame area (a), contour length (b) and coordinates of flame area centre (c and d) obtained for different states of combustion process—coal with 20% content of biomass.

The studies have shown that possible unstable combustion rely to optical parameters (e.g. flame area, contour length and flame centre coordinates), similarly to higher excess air coefficients, regardless the thermal power (**Figures 2** and **3**). The more biomass was added (**Figure 3**), the sudden changes of the discussed parameters were observed. This indicates that unstable combustion is a serious problem.

The way the flame area was defined, directly influences on the achieved quantitative parameter values of the flame area and its contour length. Mounting the camera perpendicularly to the burner axis allowed to estimate vital information about combustion process state [44–48]. These were the distance between burner and flame ignition point [45, 48] as well as spread angle of the flame. In industrial practice for full-scale power boilers, it is hard to install the camera close to a burner, because it involves disturbances in the boiler shield. So, the alternative camera set-up was tested.

## 5. Robust adaptive control of co-combustion process, using optical signals

For the proper boiler's power operation, the opportunity to assess the quality of combustion is critical [49]. The combustion flow in layers influences on the speed of chemical reactions, heat

transfer efficiency, flame stability and the generation of $NO_x$ and CO. According to sources [49–51], the type of burner, fuel type and the control method have the crucial effect on the formation of combustion aerodynamics.

Low-emission burners use the reducing properties of enriched flame by the organisation of under stoichiometric combustion zones using air or fuel staging. However, it should be noted that dust excess conditions may deteriorate and increase the unburnt loss.

Considering both environmental aspects and factors mentioned above, there is a need for a novel combustion process control system. Its specific requirements are based on the use of combustion information obtained both from conventional instrumentation and innovative techniques.

Ensuring the flame stability and the fault states, detection seems to be the most important parameters from the technological point of view. It affected the use of video technology and fibre-optic probes to complete the diagnostic information about the flame for the control system. In order to provide online, normative, emission constraints, the quantitative information on the concentration of nitrogen oxides ($NO_x$), carbon oxides (CO) and sulphur dioxide ($SO_2$) is equally important. Apart from the importance of the process state appropriate parameters selection, the selection and placement of measuring devices in such difficult industrial conditions stand a separate issue.

The change of the co-combustion process organisation stands the most popular $NO_x$ emissions reducing method. However, it causes negative consequences for the boiler operation. This results in the higher unburnt loss, increased CO emissions, the increased slagging, evaporator corrosion and instability of the flame.

Due to the fact that these phenomena are undesirable or even dangerous for the boiler, it is very difficult to achieve $NO_x$ reduction at an appropriate level. Introducing the appropriate monitoring and control system can be a solution to the problem. The advanced combustion control systems introduce additional structural modifications and signals in the form of separate air flow to individual burners, OFA nozzles and mill load or additional signals from the exhaust gas analysers such as $NO_x$, CO, and $SO_2$. Due to the fact that the excess air determines the amount of $NO_x$ generated in the coal boiler energy [49, 52], the combustion process control in a single burner would be the advantage.

The combustion process occurring in chemical reactions and physical processes can be reflected via radiation emitted by the flame. In the current state of the art, non-delayed and spatially selective additional information about the ongoing combustion process can be delivered non-invasively only using optical or acoustic diagnostic methods. It is possible to include determination of the air-fuel ratio, the quantity of heat release and temperature regarding the spectrum of flames in the visible emission. The image processing-based approach seems to be particularly important, because still and the apparent position of the flame stands the result of a dynamic equilibrium between the local flame propagation speed and the speed of the incoming fuel mixture. On this basis, it is assumed that the flame front position changes may be an indicator of this balance imminent distortion, occurring under certain conditions [53–56].

A potential problem of complex control systems, for example, the combustion process, is difficult (and thus is not full) measuring the physical-chemical quantities. In the proposed solution, a classical approach is supplemented with information about the image parameters flame, registered a high-speed camera.

As a result, the analyses highlighted the relationship between the parameters that describe the variation of the flame and the temperature of the exhaust gas in the chamber or the amount of air flow in the secondary factor. Thus, if the temperature is slowly varying size, having an inert nature, the synthesis of the controller can be used quick-picture (actually a parameter or group of the image parameters).

Primary air is used mainly for delivering pulverised coal to the burner nozzle, whereas secondary air is used for regulation purposes. Input parameters, such as the coal-biomass mixture and air flows, were changed several times during the tests to create various combustion states.

Due to the incomplete knowledge of the control object or its rapid changes in performance, the adaptive control seems to be a reasonable approach.

The nonlinear autoregressive network with exogenous inputs (NARX) is a recurrent dynamic network, with feedback connections enclosing several layers of the network. The NARX model is based on the linear ARX model, which is commonly used in time-series modelling. The defining equation for the NARX model is as follows:

$$y(t) = f\big(y(t-1), \ldots, y\big(t-n_y\big), u(t-1), \ldots, y(t-n_u)\big), \tag{9}$$

where the next value of the dependent output signal $y(t)$ is regressed on previous values of the output signal and previous values of an independent (exogenous) input signal. The NARX model can be implemented using a feedforward neural network to approximate the function $f$. This implementation also allows for a vector ARX model, where the input and output can be multidimensional.

The output of the NARX network can be considered as an estimate of the output of the modelled nonlinear dynamic system. The output is fed back to the input of the feedforward neural network as part of the standard NARX architecture. Regarding to the fact that the true output is available during the training of the network, it is possible to create a series-parallel architecture (see [56]), in which the true output is used instead of feeding back the estimated output.

The custom architecture used for further analyses is the model reference adaptive control (MRAC) system. Such a model reference control architecture has two subnetworks (see **Figure 4**). One subnetwork is the model of the plant to be controlled. The other subnetwork is the controller. Obtaining the trained NARX plant model, it is possible to create the total MRAC system and insert the NARX model inside and then add the feedback connections to the feedforward network. The next stage was focused on training of controller subnetwork.

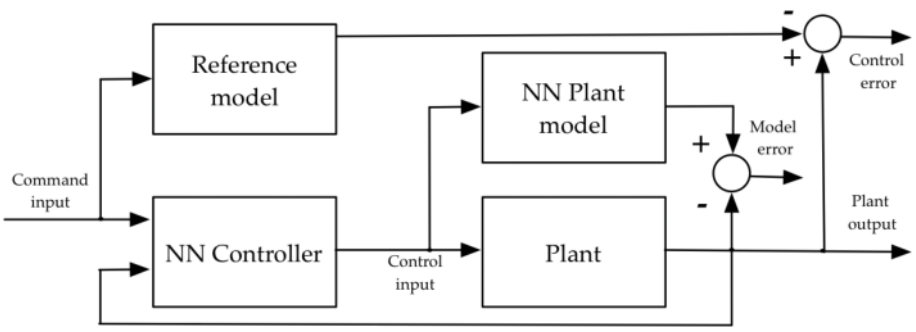


**Figure 4.** MRAC control scheme.

In order to make the closed-loop MRAC system responding in the same way as the reference model (used to generate data), the weights from the trained plant model network ought to be inserted into the appropriate location of the MRAC system. Then to achieve plant an initial input of zero, the output weights of the controller network were set to zero.

The training of the MRAC system took much longer than the training of the NARX plant model regarding to the fact that the network is recurrent and dynamic backpropagation was used. After the network was trained, it was tested by applying a test input to the MRAC network.

There were two MRAC systems designed and compared. The first one used non-optic, measurement-based set of input vectors, respectively quantitatively describe the flow of secondary air, fuel expense and vectors describing respectively exhaust temperature in the chamber, recorded in the first measurement point. The second scheme used secondary air flow control signal and chosen flame image descriptors (Otsu's method based - flame surface area and contour length).

**Figure 5** shows system response to the system reference input in both cases: with classic measurements (a) and when a flame image descriptor contour length vector was applied (b).

Simulation results shown in **Figure 5** reveal that the plant model output does follow the reference input with the correct critically damped response, even though the input sequence was not the same as the input sequence in the training data. The steady state response is not perfect for each step, but this could be improved with a larger training set and perhaps more hidden neurons. From the obtained results of the proposed neural adaptive controls, it can be concluded that control signals are bounded, abrupt changes of system parameters involve sudden changes of amplitudes of command laws and the outputs of the controlled system.

As mentioned before, imposing constraints can be a way of guaranteeing robustness. The analysed control system was evaluated by simulating a sudden step change of the load request. This test replicates the critical situation that occurs when an unexpected change of power and $NO_x$ radicals takes place. The results are presented in **Figure 6**.

The constraints are satisfied because algorithm checked all possible values of the uncertainties.

http://dx.doi.org/10.5772/intechopen.71576

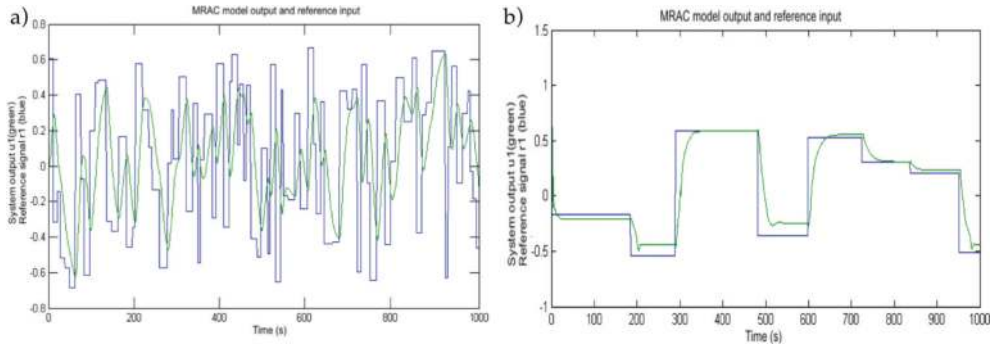


**Figure 5.** MRAC system response to the system reference input: (a) without additional information from optical signals and (b) with flame image descriptor signal included in the control scheme.

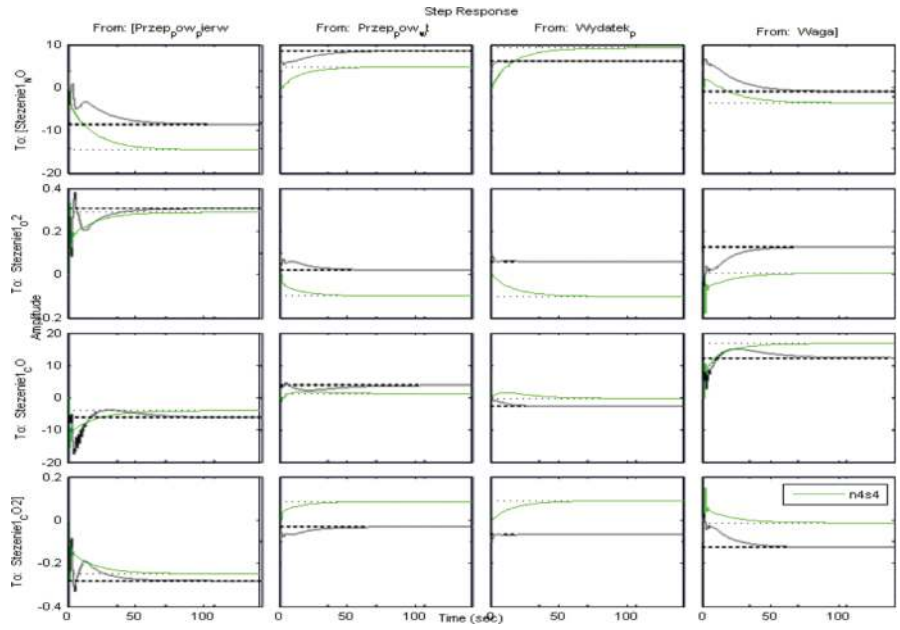


**Figure 6.** MIMO controller response to sudden change of power load regarding to the relationship between the concentrations of $NO_x$, CO, flue gas temperature in the combustion chamber for two reference models m1 and m2.

## 6. Conclusion

The flame area can be one of the crucial pointers of combustion process state [43–49, 57]. Therefore, it can be easily estimated in a series of images and it could be used in real-time applications regardless the place of camera mounting. Investigated factors used for combustion

process assessment cannot be used directly in full-scale combustion facilities, due to the fact that they strongly depend on the burner type and size of combustion chamber.

Radicals ($NO_x$, CO and $SO_2$) emission requirements are becoming more restrictive. As a result, the optimum control of combustion using low-carbon technologies seems to be very important.

The paper covered the conditions for the development of the combustion process control system as well as elaborated optimal algorithm. The aim of the algorithm was to optimise the boiler operation based on information obtained from conventional instrumentation and incorporate innovative techniques to assess the quality of the process.

The correction signals introduced by the optimising algorithm are indeed small. The proposed simulation of the MIMO controller results in better, robust performance. The evaluation of the control signals indicates a negligible change in magnitude of input signals. Consideration of uncertainties can be a considerable interest. If a model predictive controller takes into account the constraints are used, it will solve the problem, keeping the expected values of the output signals within the feasible region, but due to the external perturbations or uncertainties, this does not guarantee that any output is going to be bound. In case of uncertainties, MPC minimises the objective function for the worst situation and keeps the value of the variables within the constraint region for possible cases of uncertainties.

The increment of the prediction horizon $n$ allows better performance since a greater prediction of the future error is possible. While applying temperature values, its error weight must be high regarding to the fact that the classical temperature regulation is slow and responsible for overall performance. Too big value of the control horizon returns undesired oscillations.

As it was mentioned before, biomass co-combustion process is difficult to control. Research on using the presented approach extends the possibilities of modern combustion processes and makes them more flexible to maintain.

## Author details

Konrad Gromaszek* and Andrzej Kotyra

*Address all correspondence to: k.gromaszek@pollub.pl

Institute of Electronics and Information Technology, Lublin University of Technology, Lublin, Poland

## References

[1] Li ZQ, Jin Y. Numerical simulation of pulverized coal combustion and NO formation. Chemical Engineering Science. 2003;**58**(1):5161-5171

[2] Hein K, Bemtgen J. EU clean coal technology—Co-combustion of coal and biomass. Fuel Processing Technology. 1998;**45**:159-169

[3] Kotyra A, Wójcik W, Golec T. Chapter 84. Assessment of the combustion of biomass and pulverized coal by combining principal component analysis and image processing techniques. In: Environmental Engineering III, CRC Press. London 2010:575-579

[4] Lunze J. Robust Multivariable Feedback Control. Prentice-Hall. 1991:749-750

[5] Camacho E, Bordons C. Model Predictive Control. London: Springer. 2005:217-245

[6] Bazaraa M, Shetty C. Nonlinear programming: Theory and algorithms. Wiley-Interscience. 2013:35-167

[7] Campo P, Moriari M. Robust Model Predictive Control. Minneapolis, Minnesota: American Control Conference; 1987. p. 215-262

[8] Clarke D, Alwright JC. Chapter 19. Min-max Model-Based Predictive Control. In: Advances in model-based predictive control. In: Advances in model-based predictive control. London: Oxford University Press. 1994:221-535

[9] Mayne DQ, Rawlings J, Rao C, Scokaert P. Constrained model predictive control: Stability and optimality. Automatica. 2000;**36**:789-814

[10] Cambion G, Bastin G. Indirect adaptive state feedback control of linearly parameterized nonlinear systems. International Journal of Adaptive Control and Signal Processing. 1990;**4**:345-358

[11] Kanellakopoulos I, Kokotovic P, Marino R. An extended direct scheme for robust adaptive nonlinear control. Automatica. 1991;**27**:247-255

[12] Sastry S, Isidori A. Adaptive control of linearizable systems. IEEE Transactions on Automatic Control. 1989;**34**:405-412

[13] Kanellakopoulos I, Kokotovic P, Morse A. Systematic design of adaptive controllers for feedback linearizable systems. IEEE Transactions on Automatic Control. 1991;**36**:1241-1253

[14] Krstic M, Kanellakopoulos I, Kokotovic P. Nonlinear and Adaptive Control Design. New York: Wiley. 1995:321-563

[15] Seto D, Annaswamy A, Baillieul J. Adaptive control of nonlinear systems with a triangular structure. IEEE Transactions on Automatic Control. 1994;**39**:1411-1428

[16] Freeman R, Kokotovic P. Inverse optimality in robust stabilization. SIAM Journal on Control and Optimization. 1996;**34**(4):1365-1391

[17] Lin Y, Sontag E. Control Lyapunov universal formulae for restricted inputs. Control Theory and Advanced Technology. 1995;**10**:1981-2004

[18] Sontag E. A universal construction of Arstein's theorem on nonlinear stabilization. Systems and Control Letters. 1998;**13**(2):117-123

[19] Tsinias J. Sufficient Lyapunov-like conditions for stabilization. Mathematics of Control, Signals, and Systems. 2005;**2**(4):343-357

[20] Krstic M, Kokotovic P. Adaptive nonlinear design with controller-identifier separation and swapping. IEEE Transactions on Automatic Control. 2004;**40**:426-440

[21] Kosmatopoulos E. Universal stabilization using control Lyapunov functions, adaptive derivative feedback and neural network approximators. IEEE Transactions on Systems, Man, and Cybernetics, Part B. 2001;**28B**:472-477

[22] Kosmatopoulos E, Ioannou P. A switching adaptive controller for feedback linearizable systems. IEEE Transactions on Automatic Control. 1999;**44**:742-750

[23] Kosmatopoulos E, Ioannou P. Robust switching adaptive control of multi-input nonlinear systems. IEEE Transcations on Automatic Control. 2002;**47**(4):610-624

[24] Lin Y, Sontag E, Wang Y. A smooth converse Lyapunov theorem for robust stability. SIAM Journal on Control and Optimization. 1996;**34**:124-160

[25] Wang L, Mendel J. Fuzzy basis functions, universal approximation, and orthogonal least squares learning. IEEE Transactions on Neural Networks. 1992;**3**(5):807-814

[26] Wang L. Adaptive Fuzzy System and Control: Design and stability Analysis. NewYork: PTR Prentice Hall. 1994:75-232

[27] Chiu C. Robust adaptive control of uncertain MIMO non-linear systems—Feedforward Takagi–Sugeno fuzzy approximation based approach. IEE Proceedings—Control Theory and Applications. 2005;**152**(2):157-164

[28] Chen B, Lee C, Chang Y. Tracking design of uncertain nonlinear SISO systems: Adaptive fuzzy approach. IEEE Transactions on Fuzzy Systems. 1996;**4**:32-43

[29] Lee H, Tomizuka M. Robust adaptive control using a universal approximator for SISO nonlinear systems. IEEE Transactions on Fuzzy Systems. 2000;**8**:95-106

[30] Ying H. Sufficient conditions on uniform approximation of multivariate functions by general Takagi-Sugeno fuzzy systems with linear rule consequent. IEEE Transactions on Systems, Man, and Cybernetics, Part B. 1998;**28**(4):515-520

[31] Tsay D, Chung H, Lee C. The adaptive control of nonlinear systems using the Sugeno-type of fuzzy logic. IEEE Transactions on Fuzzy Systems. 1999;**7**:225-229

[32] Chen J, Wong C. Implementation of the Takagi-Sugeno model-based fuzzy control using an adaptive gain controller. IEE Proceedings—Control Theory and Applications. 2000; **147**(5):509-514

[33] Golea N, Golea A, Kadjoudj M: Fuzzy approximation-based model reference adaptive control of nonlinear systems. Proceedings of IEEE Conference on Control Technology and Applications 2003. p. 836-840

[34] Gao Y, Er M: Adaptive intelligent control of MIMO nonlinear systems based on generalized fuzzy neural network. Proceedings of IEEE Conference on Neural Networks. 2002. p. 2333-2338

[35] Lin W, Chen C. Robust adaptive sliding mode control using fuzzy modelling for a class of uncertain MIMO nonlinear systems. IEE Proceedings—Control Theory and Applications. 2002;**149**(3):193-201

[36] Li H, Tong S. A hybrid adaptive fuzzy control for a class of nonlinear MIMO systems. IEEE Transactions on Fuzzy Systems. 2003;**11**(1):24-34

[37] Golea N, Golea A, Benmahammed K. Fuzzy model reference adaptive control. IEEE Transactions on Fuzzy Systems. 2002;**10**(4):436-444

[38] Ordonez R, Passino K. Stable multi-input multi-output adaptive fuzzy/neural control. IEEE Transactions on Fuzzy Systems. 1999;**7**(3):345-353

[39] Chang Y, Chen B. Robust tracking designs for both holonomic and non-holonomic constrained mechanical systems: Adaptive fuzzy approach. IEEE Transactions on Fuzzy Systems. 2000;**8**:46-66

[40] Lian K, Chiu C, Liu P. Semi-decentralized adaptive fuzzy control for co-operative multi-robot systems with H 1 motion/ internal force tracking performance. IEEE Transactions on Systems, Man, and Cybernetics, Part B. 2002;**32**:269-280

[41] Er M, Gao Y. Robust adaptive control of robot manipulators using generalized fuzzy neural networks. IEEE Transactions on Industrial Electronics. 2003;**50**:620-628

[42] Marques J, Jorge M. Visual inspection of a combustion process in a thermoelectric plant, Signal Processing. Amsterdam: Elsevier. 2000;**80**:1577-1589

[43] Kotyra A, Wojcik W, Gromaszek K, Smolarz A. Biomass-coal combustion characterization based on series of flame images. Actual Problems of Economics. 2013;**5**:300-310

[44] Lu G, Gilbert G, Yan Y. Vision based monitoring and characterization of combustion flames. Journal of Physics: Conference Series. 2005;**15**:194-200

[45] Lu G. Impact of co-firing coal and biomass on flame. Fuel. 2008;**87**:1133-1140

[46] Demirbaş A. Sustainable co-firing of biomass with coal. Energy Conversion and Management. 2003;**44**:1465-1479

[47] Shaohua M. An approach of combustion diagnosis in boiler furnace based on phase space reconstruction. Proceedings of the International Conference on Intelligent Computing ICIC. 2007;**27**:528-535

[48] Su S, Pohl J, Holcombe D, Hart J. Techniques to determine ignition, flame stability and burnout of blended coals in p.f. power station boilers. Progress in Energy and Combustion Science. 2001;**27**:79-98

[49] Kordylewski W. Spalanie i paliwa (in Polish), Oficyna Wydawnicza Politechniki Wrocławskiej. Wrocław 2008:399-445

[50] Wojcik W, Kotyra A. Wykorzystanie obrazu płomienia do oceny stabilności spalania mieszanin pyłu węglowego i biomasy (in Polish). Pomiary Automatyka Kontrola. 2005;**3**: 34-36

[51] Kordylewski W. Niskoemisyjne techniki spalania w energetyce. OWPW. 2000:57-179

[52] Janiszowski K. Identyfikacja modeli parametrycznych w przykładach (in Polish). EXIT. 2002:125-142

[53] Hii N, Tan C, Alex Z, Chong W. The Measurement of Pulverised Fuel Flows by High Frequency Acoustic Emission Techniques, 7INFUB, 326–338

[54] Romero C, Li X, Keyvan S, Rossow R. Spectrometer-based combustion monitoring for fame stoichiometry and temperature control. Applied Thermal Engineering. 2005;**25**:659-676

[55] Lu G, Yan Y, Cornwell S, Riley G. Temperature profiling of pulverised coal flames using multi-colour Pyrometric and digital imaging techniques. IMTC 2005—Instrumentation and Measurement Technology Conference. 2005:1658-1662

[56] Kauranen P, Anderson-Engels S, Svanberg S. Spatial mapping of flame radical emission using a spectroscopic multi-colour imaging system. Applied Physics. 1991;**53**(4):260-264

[57] Marques J, Jorge M. Visual inspection of a combustion process in a thermoelectric plant. Signal Processing. 2010;**80**:1577-1589